RAPID GPS-BASED DETERMINATION OF EARTHQUAKE DISPLACEMENT FIELD AND MAGNITUDE FOR TSUNAMI PROPAGATION MODELING AND WARNING

*H.-P. Plag, G. Blewitt, W. Hammond, C. Kreemer**

University of Nevada, Reno
Nevada Bureau of Mines and Geology
and Seismological Laboratory
Mail Stop 178; Reno, NV 89557, USA

Y. Bar-Sever†

Jet Propulsion Laboratory,
4800 Oak Grove Drive
Pasadena, CA 91109-8099, USA

1. INTRODUCTION

Reliable tsunami early warning requires a rapid assessment of the tsunamigenic potential of an earthquake as well as a prediction of the likely propagation pattern of the tsunami. For ocean-wide tsunamis, the first hour is critical. For some coastal areas in the vicinity of seismogenic faults, for example, along the Northwest coast of the U.S., decisions on warnings for the nearby coasts have to be made within order ten minutes. For large earthquakes, initial seismological magnitude estimates tend to be too low due to a saturation [1], although recent developments in rapid magnitude estimation indicate potential solutions (e.g., [2]). Estimates of the seismic moment magnitude M_w are used as an indicator of the tsunamigenic potential, but the generation of tsunamis depends on the potential and kinetic energy imparted to the ocean by rapid co-seismic displacement of the ocean bottom [3]. Low-latency knowledge of the co-seismic displacement field in the ocean could improve tsunami early warning.

Real-time processing of GPS observations has reached a level of precision that allows determination of coseismic permanent displacement at the GPS sites with low latency. GPS-based determination of M_w for the 2004 Sumatra earthquake could have provided estimates of $M_w > 9.0$ within 12 minutes of the onset of the earthquake if sufficient real-time GPS-data had been available [4], which would have given a better early indication of the tsunamigenic potential than the much lower initial seismological magnitude estimates.

We have developed a procedure for the low-latency estimation of M_w and coseismic permanent displacement field from GPS. The procedure is implemented in a prototype system, which can be used for delayed-mode studies as well as run in real time as a component of a comprehensive early warning system. The prototype is part of the *GPS-aided Real-Time Earthquake and Tsunami (GREAT) Alert System* [5]. Here we describe the methodology for estimation of M_w and coseismic permanent displacement field from real-time GPS displacements, and present the system architecture of the prototype.

2. THE FINGERPRINT METHOD

To our knowledge, a theory for the inversion of the observed coseismic permanent displacements for a source model is currently not available. However, in many geographical areas, the location of seismogenic faults are mapped and faults can be approximated by a sequence of predefined fault elements. For each fault element, the displacement field due to a unit slip

*This work has been funded by NASA Earth Surface and Interior (NNX08AE75G), NASA Decision Support Through Earth Science (NNH07ZDA001N), and United States Geological Survey (NEHRP 07HQGR0011 and 07HQGR0016).

†The work at JPL has been funded by NASA Decision Support Through Earth Science (NNH07ZDA001N).

can be computed for the east, north, and vertical displacement of the Earth surface. We denote these displacement fields as *fingerprints*. In order to represent all possible slip directions, fingerprints for dip-slip and strike-slip are needed, thus resulting in six scalar fingerprints for each fault element.

In the *fingerprint method* the displacement $\vec{X}$ (given as $(\delta e, \delta n, \delta u)$ where e, n, u are east, north, and up-displacements) observed by GPS on the Earth's surface at location $\vec{r}$ and time t is modeled by

$$\vec{X}(\vec{r},t) = \sum_{j=1}^{N} \left\{ \alpha_j \vec{A}_j(\vec{r}) + \beta_j \vec{B}_j(\vec{r}) \right\} H(t - t_{0j}(\vec{r})) + \delta\vec{X}_{\rm s}(\vec{r},t) \ , \tag{1}$$

where $\vec{A}_j$ and $\vec{B}_j$ are the fingerprint displacement vectors at location $\vec{r}$ for the j-th fault element for dip-slip and strike-slip, respectively; H is the Heaviside function; t_{0j} the predicted arrival time of the permanent displacement caused by element j at location $\vec{r}$, and $\delta\vec{X}_s$ the predicted displacements caused by seismic waves or other disturbances. α_j and β_j are the scaling factors for dip-slip and strike-slip, respectively, at the j-th fault element, which are determined in a least-squares fit of eq. 1 to a set of observed displacement time series.

The *fingerprint method* makes use of the knowledge of the approximate location of the epicenter as provided by seismological methods. This location is used to first determine the set of fault elements potentially participating in the rupture, and the set of GPS stations potentially having experienced a permanent displacement. A search is then conducted in a model space that contains all physically reasonable combinations of fault elements, which could have ruptured together during the earthquake in order to determine the "best fit" combination. Several statistical parameters of the fit are used to identify the "best fit" combination, including the variance of the GPS displacement time series explained by an element combination.

3. FINGERPRINT DATABASE

For a given fault element, fingerprints can be computed using a forward-modeling algorithm. However, computation of the displacements is demanding in cpu-time and cannot be done in the context of a real-time warning system. Therefore, in order to apply the *fingerprint method*, a database of fault elements has to be populated with fingerprints sampled with sufficiently high spatial resolution so that the displacements can be interpolated to the GPS site locations with sufficient accuracy. Several global fault databases exist and provide reasonable starting points. We used the fault database available at NOAA's Center for Tsunami Research [6], which ensures that the GREAT prototype is consistent with NOAA's tsunami warning model. This database comprises 573 fault elements for all major tsunamigenic faults in the Pacific, Indian Ocean, and Caribbean Sea. Each fault element has a length of 100 km. For each fault element, a pair of connected shallow and deep planes is defined (for details, see [6]), resulting in a total of 1,146 fault planes. For each fault element, we computed fingerprints using the algorithm by [7] for an elastic Earth model derived from PREM. In order to account for an uncertainty in the dip of the elements, we computed for each element fingerprints for several dip values, so that the total number of available fingerprints is currently about 4,500.

In order to limit the interpolation error for the GPS site displacement to $< 1\%$ and keep the size of the fingerprint files as small as possible, the fingerprints are sampled with high spatial resolution in the near-field of a fault element and much lower resolution in the far-field. We chose to sample the fingerprints for a set of circles centered around the midpoint of the element with an azimuth resolution of 2 degrees (180 points per circle). For the radius r_i of the i-th circle we established the relation

$$r_i = (x_0 + i \cdot \delta x)^3 \ ; i = 1, K \tag{2}$$

with $x_0 = 0.3$, $\delta x = 0.03$, and $K = 112$ as sufficient to keep the interpolation error below 1%. With these parameters, the total area covered by a fingerprint ranges from a radius of about 3 km to about 5,400 km. Figure 1 illustrates the variable spatial resolution of the fingerprints as precomputed for the fingerprint analysis.

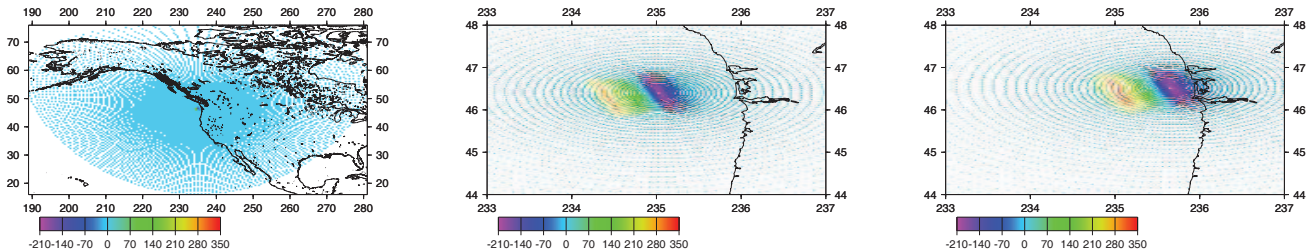

Fig. 1. Examples of fingerprints illustrating the variable spatial sampling. Left diagram: Full pattern of the fingerprint in vertical displacement for a unit dip-slip on the shallow plane of the U.S. West Coast. Middle diagram: Near-field part of the fingerprint in the left diagram. Right diagram: Near-field part of the fingerprint for the deep plane at the same location.

4. THE GPS-COMPONENT IN THE GREAT PROTOTYPE

The integration of GPS-based determination of magnitude and displacement field in a system informing decision makers is sketched in Fig. 2. In the GREAT alert system, the GDIS is designed to provide refined magnitude estimates to the decision makers as well as estimates of magnitude and displacement field to a tsunami modeling component.

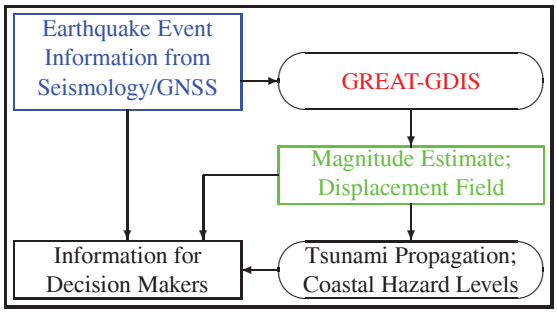

Fig. 2. High-level architecture of a tsunami early warning system integrating GPS-determined displacements. For event detection, seismological observations are used, and the approximate epicenter location and time are provided to the component for the GPS-based magnitude and displacement field estimation (GREAT-GDIS). This component requires displacement time series from a sufficiently dense regional GPS network. The estimates of the magnitude and coseismic permanent displacement field for the ocean bottom are used in the prediction of tsunami amplitude and propagation pattern in support of the decision for which coastal areas to issue a tsunami warning.

The implementation of the *fingerprint algorithm* in the GREAT-GDIS component is sketched in Figure 3. Real-time GPS displacement time series with 1 s temporal sampling as computed by the Jet Propulsion Laboratory for a global network of stations with currently on the order of 100 stations are transferred to the host by a push algorithm. The program *capture* receives these time series with a time delay < 10 s and updates an archive with these time series. The program *cleaner* improves the quality of the time series in the archive constantly by eliminating infrequent spikes and applying a sidereal filter. An event notice triggers *earthquake* to issue an alert notice for *geqdis* to initiate a fingerprint analysis. *geqdis* determines the set of GPS sites and the time window to be used in the analysis, and issues a request for time series to the *gnss-server*. While waiting for the response, *geqdis* prepares the analysis by computing all parts of the normal equations independent of the displacement time series. If the event notice was for a synthetic earthquake (used for delayed-mode sensitivity studies and assessments), *earthquake* also provides the synthetic offsets to *gnss-server*. *gnss-server* extracts the requested time series from the archive, which in real-time mode normally requires a wait until sufficient data after the onset of the earthquake have arrived. In case a synthetic earthquake is considered, *gnss-server* adds the synthetic offsets to the time series before delivering these to *geqdis*. *geqdis* then conducts the search for the "best fit" element combination. After that, it produces a message file for the tsunami propagation component, which includes the magnitude estimate and the displacement field.

None of these individual steps appears to be time critical. The main time-limiting factor is the requirement for sufficient data after the onset of the earthquake to capture the co-seismic permanent displacement at a sufficiently large number of stations. Therefore, the network density close to the rupture area is a critical design parameter for the overall system.

Figure 3 also shows the structure of the GDIS database. Major faults are specified in a *Fault* table, which helps to group the individual fault elements. It is anticipated to compare different geophysical models, and these models are collected in a *Model* table. Meta data for the available fingerprints is collected in a *Fingerprints* table linked to both models and fault elements. The

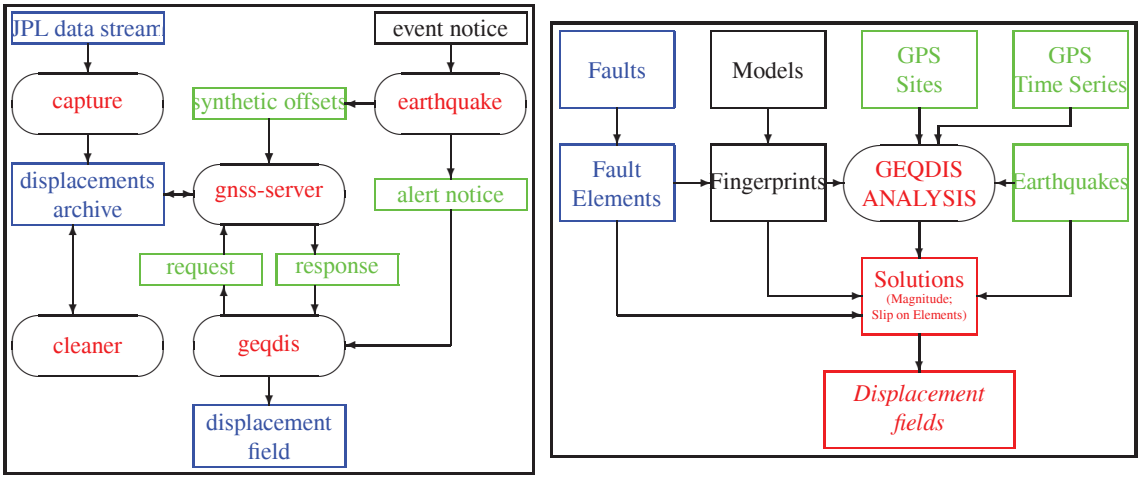

Fig. 3. Architecture of the GPS-component of the GREAT alert system (left) and structural elements of the Fingerprint analysis (right). For details, see text.

database stores information on available GPS sites in the *GPS sites* table, which is used to built the requests for GPS time series mentioned above. Finally, information on earthquakes is compiled in the *Earthquakes* table for reuse in delayed mode.

5. CONCLUSIONS AND PERSPECTIVE

The GDIS prototype has been used to demonstrates the feasibility of the *fingerprint method* for low-latency determination of moment magnitude and coseismic permanent displacement field based on real-time GPS displacement time series, and to study the robustness of the real-time implementation. The next step is the integration of this component in the GREAT alert system focusing in particular on the interface between GDIS and the tsunami propagation module.

6. REFERENCES

[1] R. Kerr, "Failure to gauge the quake crippled the warning effort," *Science*, vol. 307, pp. 201, 2005.

[2] Y.M. Wu and L. Zhao, "Magnitude estimation using the first three seconds pwave amplitude in earthquake early warning," *Geophys. Res. Lett.*, vol. 33, no. 16, pp. doi:10.1029/2006GL026871, 2006.

[3] Y. T. Song, L.-L. Fu, V. Zlotnicki, C. Hi, V. Hjorleifsdottir, C. K. Shum, and Y. Yi, "The role of horizontal impluses of the faulting continental slope in generating the 26 december 2004 tsunami," *Ocean Modeling*, vol. 20, no. 4, pp. 362–379, 2008.

[4] G. Blewitt, C. Kreemer, W. Hammond, H.-P. Plag, S. Stein, and E. Okal, "Rapid determination of earthquake magnitude using GPS for tsunami warning systems," *Geophys. Res. Lett.*, vol. 33, pp. L11309, doi:10.1029/2006GL026145, 2006.

[5] Y. Bar-Sever, R. Gross, T. Song, F. Webb, G. Blewitt, H.-P. Plag, W. Hammond, C. Kreemer, J. Sundstrom, V. Hsu, K. Hudnut, and M. Simons, "GPS-aided real-time earthquake and tsunami (GREAT) alert system," Invited presentation, AGU 2009, San Francisco, available at https://ppp.gdgps.net/, 2009.

[6] E. Gica, M. C. Spillane, V. V. Titov, C. D. Chamberlin, and J. C. Newman, "Development of the forecast propagation database for noaas short-term inundation forecast for tsunamis (sift)," NOAA technical memorandum OAR PMEL-139, Pacific Marine Environmental Laboratory, Seattle, WA, 2008.

[7] F. F. Pollitz, "Coseismic deformation from earthquake faulting on a layered spherical Earth," *Geophys. J. Int.*, vol. 125, pp. 1–14, 1996.